

See discussions, stats, and author profiles for this publication at: <https://www.researchgate.net/publication/263953524>

Reduction Kinetics of Foreign-Ion-Promoted Ilmenite Using Carbon Monoxide (CO) for Chemical Looping Combustion

ARTICLE *in* INDUSTRIAL & ENGINEERING CHEMISTRY RESEARCH · JULY 2013

Impact Factor: 2.59 · DOI: 10.1021/ie4015974

CITATIONS

7

READS

32

3 AUTHORS, INCLUDING:



Ningsheng Cai

Tsinghua University

138 PUBLICATIONS 1,797 CITATIONS

SEE PROFILE

Reduction Kinetics of Foreign-Ion-Promoted Ilmenite Using Carbon Monoxide (CO) for Chemical Looping Combustion

Jinhua Bao, Zhenshan Li,* and Ningsheng Cai

Key Laboratory for Thermal Science and Power Engineering of Ministry of Education, Beijing Municipal Key Laboratory for CO₂ Utilization & Reduction, Department of Thermal Engineering, Tsinghua University, Beijing 100084, China

ABSTRACT: In a previous work by our group, a new kind of ilmenite oxygen carrier, namely, natural ilmenite particles impregnated with foreign ions (K⁺, Na⁺, or Ca²⁺), was reported as having a promoted reactivity. The objective of this work was to investigate the detailed reduction kinetics of the new foreign-ion-promoted ilmenite carrier. Ilmenite particles impregnated with different types of foreign ions, including K⁺, Na⁺, and Ca²⁺, at different loading ratios were investigated by thermogravimetric analysis (TGA) using CO as the reducing gas. The samples tested by TGA for kinetics included the initial ilmenite particles and particles extracted from the fluidized-bed reactor after 40, 70, or 100 continuous redox cycles, as was done in the previous work. The obtained kinetic parameters were applied for the design of a chemical-looping combustion (CLC) reactor. The findings confirmed that the impregnation of foreign ions can promote the reduction rate of ilmenite. The kinetic data obtained by TGA indicated that the 15 wt % K⁺-promoted ilmenite showed a ~6.85 times faster reactivity than the activated raw ilmenite after 40 cycles in the fluidized bed. Even when the number of cycles was increased to 100, the modified ilmenite still maintained a much higher reduction rate than the activated raw ilmenite. Although the reduction rate of the 15 wt % K⁺-promoted ilmenite decreased as the CO concentration decreased, it still remained higher than the reactivity of the activated raw ilmenite. A theoretical calculation with the kinetic parameters indicated that the required minimum solids inventory of the fuel reactor was 1670 kg/MW_{th} for the 15 wt % K⁺ promoted ilmenite, which was approximately one-seventh that required for the activated raw ilmenite (11436 kg/MW_{th}).

1. INTRODUCTION

Chemical-looping combustion (CLC) typically employs an interconnected fluidized-bed system, where an oxygen carrier is employed as the bed material transferring oxygen from the air to the fuel for combustion.^{1,2} Isolation of the fuel from the air produces a flue gas primarily composed of carbon dioxide and water vapor; by condensing the steam, high-purity CO₂ can inherently be obtained. The CLC technique has been successfully demonstrated in different scaled prototype units (10 kW_{th}–3 MW_{th}) based on interconnected fluidized beds.^{3–7} The development of suitable oxygen carriers that circulate between two fluidized-bed reactors is a key issue for the performance of CLC. CLC with gaseous fuels, such as natural gas or syngas, has been widely demonstrated to be feasible with synthetic carriers.^{8–11} However, in solid-fuel CLC processes, the solid fuel undergoes thermal decomposition and gasification in the fuel reactor, producing ash. Because of the partial loss of oxygen carriers accompanying the removal of the ash from the reactors, low-cost and easily available oxygen carriers, such as natural minerals, are preferred over synthetic carriers. The identification and testing of inexpensive oxygen carriers is desirable and meaningful for the development of CLC with solid fuels.

So far, the low-cost and attractive oxygen carriers reported for solid-fuel CLC include natural Fe-, Mn-, and Cu-based ores^{12–17} and industrial residues.^{17,18} Among these oxygen carriers, ilmenite, a natural mineral composed of FeTiO₃, is considerably less expensive than synthetic materials and has been confirmed as a promising oxygen carrier for solid-fuel CLC.^{19–26} However, a significant issue with ilmenite is its low reduction reactivity. To achieve a complete conversion of

syngas in the fuel reactor, a large bed inventory is necessary, thus requiring a larger-scale unit and increasing capital costs. Therefore, improving the reactivity of ilmenite is critical.

A previous work verified that the introduction of foreign ions (K⁺, Na⁺, and Ca²⁺) into ilmenite particles can promote the ilmenite's reduction reactivity.²⁷ The enhancement of the reduction reactivity of ilmenite by foreign ions was found to occur in the order K⁺ > Na⁺ > Ca²⁺. Ilmenite impregnated with 15 wt % K⁺ was found to be the best candidate, with a reactivity enhancement reaching the same level as that provided by a synthetic Ni-based carrier. Additionally, the modified ilmenite showed a high stability in its reactivity over 40 repeated redox cycles in a fluidized-bed reactor without any agglomeration or obvious particle fragmentation.

Although the product gas distributions in the fluidized bed obtained in the previous work can reflect the reactivity of the modified ilmenite, detailed reaction kinetics cannot be obtained directly from the outlet gas composition. This is because the inlet CO fuel gas was fully oxidized into CO₂ by the modified ilmenite through a fast reaction in the fluidized bed. The reaction kinetics of the oxygen carrier determines the key parameters for the design, optimization, and scaleup of a CLC system, including the solids circulation rate between reactors and the solids inventory in each reactor. In addition, oxygen carriers experience different environments during continuous

Received: May 19, 2013

Revised: June 28, 2013

Accepted: July 12, 2013

Published: July 12, 2013

Table 1. Main Components (wt %) of Raw Ilmenite and Modified Ilmenite Analyzed by XRF and Mass Fractions (wt %) of Foreign Ions (K, Na, or Ca) with Respect to the Total Amount of Ti and Fe, Including Data on the Initial Particles and the Particles Existing after 40 and 100 Cycles in the Fluidized Bed

ilmenite	initial						40 cycles					100 cycles
	raw	10% K	10% Na	10% Ca	5% K	15% K	10% K	10% Na	10% Ca	5% K	15% K	15% K
TiO ₂	50.54	32.82	33.92	43.33	35.65	29.19	42.16	46.59	47.15	46.51	37.82	38.08
Fe ₂ O ₃	42.32	21.40	23.60	31.22	27.40	19.83	47.37	45.69	29.11	43.96	50.43	49.95
K ₂ O, Na ₂ O, CaO	—	16.82	28.74	21.73	10.31	19.01	6.04	3.02	20.24	4.40	6.99	7.00
CO ₂	—	26.40	10.91	—	23.47	29.78	—	—	—	—	—	—
K ₂ Na ₂ Ca/(Ti + Fe)	—	0.40	0.65	0.32	0.21	0.50	0.086	0.037	0.30	0.062	0.10	0.10

recirculation in the CLC reactors. Therefore, it is of practical interest to study the kinetics of the newly developed ilmenite and consider the effects of different operating conditions. Because the oxidation of ilmenite by oxygen from the air is generally fast, more attention can be paid to the reduction reactivity difference between the new ilmenite oxygen carrier and raw ilmenite. In CLC with solid fuels, the reducing gases are mainly CO and H₂ generated from char gasification ($C + CO_2 = 2CO$ and $C + H_2O = CO + H_2$). The reduction of metal oxygen carriers with H₂ is generally faster than that with CO, as summarized by Mendiara et al.²⁸ Therefore, this article focuses on the reduction kinetics of ilmenite with CO as the reducing gas.

The objective of this work was to investigate the reduction kinetics of foreign-ion-promoted ilmenite with CO as reducing gas. The effects of the gas concentration and the number of cycles were addressed. The kinetic parameters for the reduction of the promoted ilmenite oxygen carrier with CO were established based on the experimental data. Further, the kinetic parameters obtained were used to determine the solids circulation rate and solids inventory required for a CLC system working with this foreign-ion-promoted ilmenite.

2. EXPERIMENTAL SECTION

2.1. Ilmenite. The preparation of raw ilmenite and ilmenite impregnated with different foreign ions (K⁺, Na⁺, or Ca²⁺) at different loadings (5, 10, and 15 wt %) was reported in a previous work.²⁷ The raw ilmenite was preoxidized to its most oxidized state by thermally treating fresh ilmenite at 950 °C in air for 24 h.²⁹ The raw ilmenite particles had a density of 4246 kg/m³ and a surface area of 0.64 m²/g. Ilmenite modified by foreign ions was prepared through the wet impregnation method.³⁰ For simplicity, the foreign-ion-modified ilmenite samples are designated as K5-ilmenite, K10-ilmenite, K15-ilmenite, Na10-ilmenite, and Ca10-ilmenite, where K, Na, and Ca are the foreign ions, and 5, 10, and 15 denote the mass percentages of the foreign ions relative to ilmenite. All ilmenite particles used for kinetics determination were in the size range of 125–200 μm.

Table 1 lists the main components of the raw and modified ilmenites analyzed by X-ray fluorescence (XRF) and the mass fractions of foreign alkali metals to the total amount of Ti and Fe. Data for particles subjected to 40 and 100 cycles in the fluidized bed are also included. The raw ilmenite was found to contain 50.54% TiO₂, 42.32% Fe₂O₃, 2.32% SiO₂, and some other minor phases. X-ray diffraction (XRD) showed that Fe₂TiO₅ and TiO₂ were the major components, with a minor amount of Fe₂O₃. The initial K-, Na-, and Ca-modified ilmenites were mainly composed of TiO₂, Fe₂O₃, and alkali carbonate (K₂CO₃ or Na₂CO₃) or calcium oxide (CaO). After 40 continuous reduction–oxidation cycles in the fluidized bed,

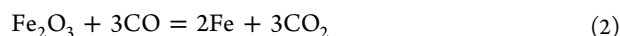
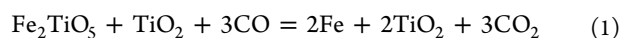
TiO₂ and Fe₂O₃ still remained as the main species in the modified ilmenite, but the forms of foreign ions K⁺ and Na⁺ changed. Both K₂CO₃ and Na₂CO₃ were found to undergo thermal decomposition with the production of K₂O and Na₂O, respectively, before the start of the first cycle. In addition, a fractional loss of K⁺ and Na⁺ occurred after cycling, which is discussed in detail in section 4.2.

2.2. Experimental Setup. A laboratory-scale fluidized-bed reactor made of quartz (i.d. = 30 mm) was used to prepare the ilmenite particles experiencing different redox cycles. In each batch, a sample of ~50 g of ilmenite particles with a size of 125–200 μm was placed on a porous plate and then fluidized at a constant gas flow rate of 2 L/min (at standard temperature and pressure, STP), giving $U/U_{mf} = 3.07$ (where U is the particle velocity and U_{mf} is the minimum fluidization velocity) at 900 °C. In each cycle, 11 vol % CO was used to reduce the bed material at 900 °C for 5 min, and 5.5 vol % O₂ (air diluted by nitrogen) was introduced for full oxidation at 840 °C, with 3 min of nitrogen purging between reduction and oxidation. Each sample underwent 40, 70, or 100 continuous redox cycles and was then extracted from the fluidized bed for reactivity tests. These experiments performed in the fluidized bed were described in detail in our previous work.²⁷ The choice of conducting the successive redox cycles in a fluidized bed, instead of a thermogravimetric analyzer, was aimed at creating a reaction environment that was more similar to a practical CLC system, that is, an interconnected fluidized-bed system. In this way, the samples prepared in the fluidized bed can be considered more representative.

A thermogravimetric analyzer (TA Q600) was used to investigate the kinetics of the reduction of the raw and foreign-ion-modified ilmenite. The analysis of each type of ilmenite included the initial particles and particles that had been subjected to different number of redox cycles in the fluidized-bed reactor. In each test, a sample of ~15 mg of oxygen carrier was loaded into an alumina pan. Initially, a 25 mL/min (STP) air flow was fed through the bypass port into the thermogravimetric analysis (TGA) reactor, mixing with 75 mL/min (STP) balance gas N₂ through gas port 1, to obtain 5.25 vol % O₂/N₂. At the same time, the temperature was increased abruptly (heating rate of ~258 °C/min) to the reaction temperature (900 °C) and then held constant. The 5.25 vol % O₂/N₂ mixture was maintained for 15 min to ensure that the sample was fully oxidized at the start. After oxidation, the TGA reactor was purged with 100 mL/min (STP) N₂ for 10 min. Then, a 100 mL/min (STP) flow of 11 vol % CO/N₂ was fed through gas port 2 as a reductant for 60 min, followed by another 10-min N₂ purge. Finally, the reduced oxygen carrier was fully oxidized by a flow of 5.25 vol % O₂/N₂ for 20 min. The TGA reactor was cooled to room temperature under an atmosphere of N₂. Here, the use of 11 vol % CO for

reduction and 5.25 vol % O₂ for oxidation was for consistency with the fluidized-bed experimental conditions used in our previous work.²⁷ To examine the effect of the reducing-gas concentration on the reactivity, several experiments were carried out at 900 °C with different CO concentrations (11, 7, 5, 3, and 1 vol %). CO concentrations lower than 11 vol % were obtained by diluting the standard 11 vol % CO/N₂ gas (switch to bypass port) with balance N₂ gas (gas port 1) at different flow-rate ratios with a constant mixed flow rate of 100 mL/min (STP). At this time, air from gas port 2 was used for oxidization. It should be mentioned that the reason for switching the reducing gas from gas port 2 to the bypass port was that gas ports 1 and 2 could not be activated at the same time.

2.3. Data Evaluation. According to mass balance calculations, the final reduction state of iron for most of the ilmenite oxygen carriers, especially K- and Na-modified ilmenites, was between Fe²⁺ and Fe⁰ after reduction with 11 vol % CO for 60 min in the TGA reactor. Reduction of the ilmenite components, Fe₂TiO₅ and Fe₂O₃, by CO can be summarized by the equations



The conversion of the ilmenite oxygen carrier, X_r , during reduction in the TGA reactor was calculated as

$$X_r = \frac{m_0 - m_t}{m_0 R_o} \quad (3)$$

where m_0 is the initial mass of the tested sample at $t = 0$ and m_t is the mass at time t . R_o is the oxygen ratio of the carrier and signifies the mass fraction of oxygen in the fully oxidized carrier, calculated as

$$R_o = \frac{m_o - m_r}{m_o} \quad (4)$$

where m_o and m_r are the masses of the most oxidized and reduced forms, respectively, of the ilmenite. R_o is equal to 15 wt % in theory on the basis of the transformation from Fe³⁺ to Fe⁰.

3. MATHEMATICAL MODEL FOR REDUCTION KINETICS

The reduction of ilmenite oxygen carrier by CO is a typical noncatalytic gas–solid reaction that includes the following elementary steps: (1) external mass transfer of CO from the gas phase to the particle surface, (2) internal mass transfer of CO or CO₂ inside the pores of the particle, (3) adsorption of CO on the pore surface, (4) ion diffusion through the solid product layer, and (5) chemical reaction at the reactant surface. Resistance from each of these steps can affect the reduction rate. The external mass-transfer resistance was reduced as much as possible in this work by using high gas flow rates and small sample masses in the TGA reactor. Moreover, as the reduction continued, the porosity of the ilmenite particles increased because of the lower molar densities of Fe₃O₄, FeO, and Fe compared to that of Fe₂O₃. Even so, for ilmenite oxygen carrier, the micropore and mesopore characteristics can affect the internal diffusion, so that the particle size of ilmenite can have some effect on the internal mass transfer. In this work, all particle sizes were kept constant in the range of 125–200 μm. Therefore, the effect of particle size on internal diffusion was not considered separately, being included in the apparent

reaction term instead. When ilmenite is reduced by CO, the formation and growth of the solid product occurs at the interface between the solid reactant and the solid product. Therefore, it becomes more difficult for CO to make contact with the reactant surface. Further reduction thus depends on the type of migrating species, which can occur at either the reactant–product interface (inward transport of CO) or the product–gas interface (outward transport of oxygen ions). Considering that the transport of CO through the solid product layer is relatively difficult, it can be assumed that only oxygen ions diffuse outwardly³¹ and the reaction takes place at the product–gas interface. CO from the gas phase is adsorbed and then reacts with oxygen ion, generating CO₂. Therefore, the reduction reactivity is controlled by both the oxygen diffusion through the product layer and the chemical reaction. Different gas–solid reaction models have been proposed for kinetic predictions, as summarized by Adanez et al.³² The shrinking-core model assumes that the particle is a nonporous sphere and that the solid product layer grows on the outside surface of the solid reactant.³³ The grain model with a spherical or platelike geometry of the grain assumes that the chemical reaction controls the global reaction rate.³⁴ The random-pore model (RPM) was initially applied to a gas–solid reaction by Bhatia and Perlmutter.³⁵ Recently, Liu et al.³⁶ also used the random-pore model to describe the kinetic behavior of oxygen carriers. The nucleation and growth model has been applied to some gas–solid reactions, with the solid conversion presenting a sigmoidal curve as a function of time.³⁷ Previous studies of ilmenite have extensively demonstrated that the reduction rate of ilmenite is affected by both the reaction temperature and the fuel gas concentration.^{19–26} The mathematical model developed in this work was merely for the purpose of fitting the experimental data and facilitating subsequent reactor design and is not a mechanism model for kinetics. Therefore, the kinetics model of the reduction of the ilmenite were assumed to follow the semiempirical equation

$$\frac{dX_r}{dt} = k(1 - X_r)^n C_{\text{CO}}^m \quad (5)$$

where X_r and dX_r/dt (1/s) are the conversion ratio and conversion rate, respectively, of the oxygen carrier; C_{CO} (mol/m³) denotes the CO concentration; k [m³/(mol·s)] is the coefficient of the apparent chemical reaction rate; and m is the reaction order. As the reduction proceeded, the surface area of the solid reactant available for the reactive gas changed. This change can be attributed to the nucleation and growth of the solid product, along with the formation of islands of solid product.³⁸ The variation of the available surface area influences the reduction rate. Here, for simplicity, $(1 - X_r)^n$, where n is an empirical parameter, was used to represent the effect of the change of the surface area on the reduction rate. The parameters k , n , and m were obtained by fitting the calculated conversion ratio to the experimental data. Table 2 lists the kinetic parameters for the reduction of different types of ilmenite (both initial and 40-cycled) with 11 vol % CO at 900 °C. Because k refers to the apparent chemical reaction rate, it is related to the surface area of the reactant particle. As the number of cycles increased, the surface areas and pore volumes of the activated raw ilmenite and the ilmenites modified with 10 wt % K, 10 wt % Na, and 15 wt % K all increased, as reported previously.²⁷ Correspondingly, these types of ilmenites showed an increase in k after 40 cycles, as seen in Table 2. Table 3 reports the kinetic parameters for the reduction of K15-ilmenite

Table 2. Kinetic Parameters for Ilmenite Reduction with 11 vol % CO at 900 °C for Raw Ilmenite and Ilmenite Impregnated with 10% K, 10% Na, 10% Ca, 5% K, and 15% K Initially and after 40 Cycles in the Fluidized Bed $m = 1$

ilmenite	initial		after 40 cycles	
	$k [\times 10^{-4} \text{ m}^3/(\text{mol}\cdot\text{s})]$	n	$k [\times 10^{-4} \text{ m}^3/(\text{mol}\cdot\text{s})]$	n
raw ^a	0.56	0.67	1.25	1
			0.67	1.4
10% K	5.01	1.6	8.62	2
10% Na	2.64	1.6	4.87	2
10% Ca ^a	3.06	2	2.78	2
	6.26	1.2	1.25	1.2
5% K	4.94	1.5	4.45	1.5
15% K	5.01	1.6	9.04	2

^aFor raw ilmenite after 40 cycles and Ca10-ilmenite, top row, $\text{Fe}_2\text{O}_3 \rightarrow \text{Fe}_3\text{O}_4$; bottom row, $\text{Fe}_3\text{O}_4 \rightarrow$.

Table 3. Kinetic Parameters for the Reduction of 40-Cycled K15-Ilmenite at 900 °C with Different CO Concentrations $m = 1$

CO content (vol %)	CO concentration (mol/m ³)	$k [\times 10^{-4} \text{ m}^3/(\text{mol}\cdot\text{s})]$	n
11	1.14	9.04	2
7 ^a	0.73	9.04	1
		9.04	7
5 ^a	0.52	6.95	2
		9.04	8
3 ^a	0.31	9.04	2
		9.04	5
1	0.10	11.8	1

^aFor CO contents of 3–7 vol %, top row, $\text{Fe}_2\text{O}_3 \rightarrow \text{Fe}_3\text{O}_4$; bottom row, $\text{Fe}_3\text{O}_4 \rightarrow$.

(40-cycled) at 900 °C with different CO concentrations. The conversions of the ilmenite carriers predicted with these kinetic parameters are included in section 4, along with the experimental results from TGA.

The average conversion rate ($\overline{dX_r/dt}$) (1/s) within a period of time Δt (s) was calculated as

$$\overline{dX_r/dt} = \frac{\int_0^{\Delta t} \frac{dX_r}{dt} dt}{\Delta t} \quad (6)$$

4. RESULTS AND DISCUSSION

4.1. Effect of Foreign Ion Type. The reduction reactivities of raw ilmenite and ilmenite impregnated with different types of foreign ions (K^+ , Na^+ , and Ca^{2+}) were investigated by TGA with 11 vol % CO at 900 °C. Both initial carrier particles and particles extracted from the fluidized bed after 40 continuous cycles were tested. Figure 1 shows the conversions of the oxygen carriers with time and the relevant conversion rates as functions of conversion. Here, the conversion rate was calculated according to eq 5. Thermodynamically, only the reduction from Fe_2O_3 to Fe_3O_4 gives complete combustion of CO to CO_2 ; further reduction past Fe_3O_4 results in a low CO_2 concentration diluted by unconverted CO at the outlet of the fuel reactor. Hence, CLC usually involves operation between Fe_2O_3 and Fe_3O_4 . Accordingly, only the conversion rate during the transition from Fe_2O_3 to Fe_3O_4 ($X_r = 0 \rightarrow 0.11$) is plotted in Figure 1b, whereas the latter is plotted in Figures 2b and 3b.

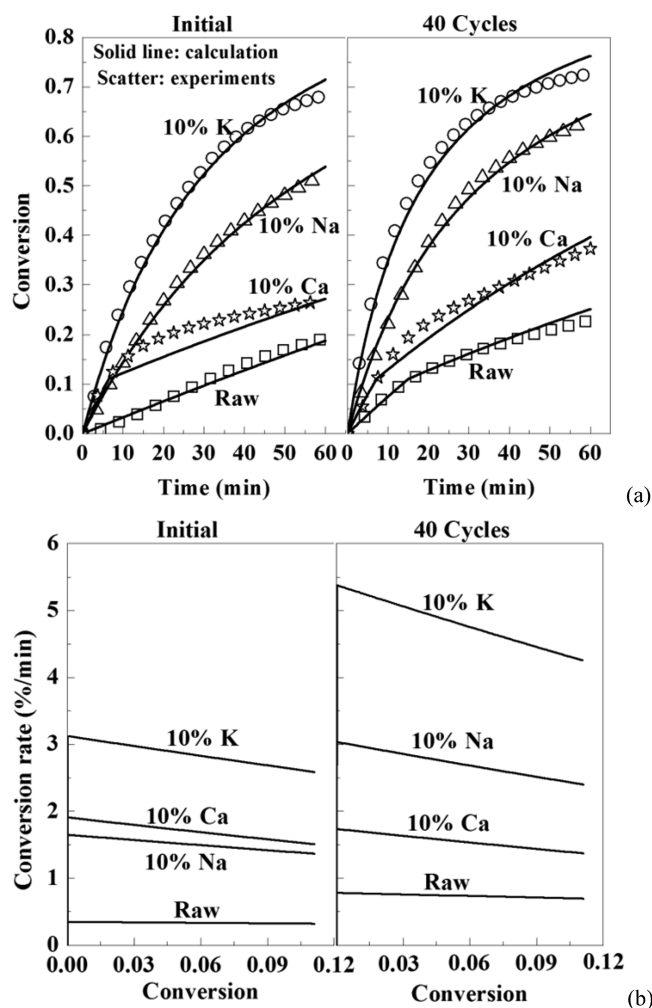


Figure 1. Reduction reactivity comparison between raw ilmenite and ilmenite impregnated with 10% K, 10% Na, or 10% Ca with 11 vol % CO at 900 °C in a TGA reactor. (a) Conversion of the oxygen carrier with time and (b) conversion rate during the reduction from Fe_2O_3 to Fe_3O_4 ($X_r = 0 \rightarrow 0.11$) in ilmenite as a function of conversion. Both the initial carrier and the carrier after 40 cycles in the fluidized bed are presented.

Figure 1 shows that the foreign-ion-modified ilmenite provided faster reactivity than the raw ilmenite, both initially and after 40 cycles. The reactivity-promoting effect of the tested foreign ions was found to be in the order $\text{K}^+ > \text{Na}^+ > \text{Ca}^{2+}$ during the entire reduction, except for the first 9.4 min, when Ca10-ilmenite exhibited a slightly faster reactivity than Na10-ilmenite. The small difference between initial Ca10-ilmenite and Na10-ilmenite can be found from Figure 1b. In Figure 1b, during the reduction to Fe_3O_4 , the conversion rate of the initial Ca10-ilmenite varied in the range of 1.51–1.91%/min, which is slightly higher than that of Na10-ilmenite (1.36–1.65%/min). In addition, the reactivity changed over the 40 cycles in the fluidized bed, as seen in Figure 1a,b. Raw ilmenite obtained a faster reactivity due to the activation process, increasing from 0.33%/min to 0.74%/min on average (eq 6). The reactivities of the K- and Na-modified ilmenites also increased after 40 cycles; however, their reactivity increases were far greater than that of raw ilmenite. Specifically, the reduction rate of K10-ilmenite increased from 2.59–3.12%/min to 4.25–5.37%/min; the reduction rate of Na10-ilmenite increased from 1.36–1.65%/min to 2.40–3.03%/min. Unlike the K- and Na-modified

ilmenites, Ca10-ilmenite did not exhibit an enhanced reactivity after 40 cycles, but its reactivity was still faster than that of the activated raw ilmenite. The reactivities of the 40-cycled ilmenites impregnated with 10 wt % K, 10 wt % Na, and 10 wt % Ca were, on average, 6.53, 3.69, and 2.11 times faster than that of the activated raw ilmenite. This result demonstrates that the low reactivity of natural ilmenite can be promoted by impregnating the ilmenite particles with foreign ions. Additionally, among the foreign ions tested, K^+ was found to be the best option for improving the ilmenite reactivity.

4.2. Effect of K^+ Loading. To determine the optimum K^+ loading, the reactivity of ilmenite impregnated with different mass ratios of K^+ was studied by TGA with 11 vol % CO at 900 °C. Figure 2 compares the reduction reactivities of ilmenite

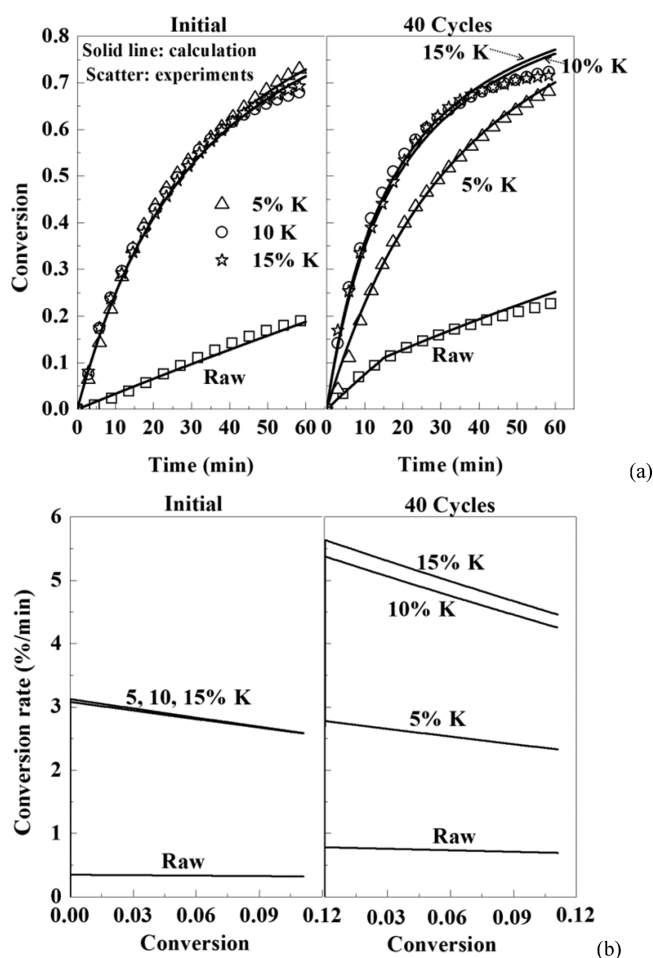


Figure 2. Reduction reactivity comparison between raw ilmenite and ilmenite impregnated with 5%, 10%, or 15% K with 11 vol % CO at 900 °C in a TGA reactor. (a) Conversion of the oxygen carrier with time and (b) conversion rate during the reduction from Fe_2O_3 to Fe_3O_4 ($X_r = 0 \rightarrow 0.11$) in ilmenite as a function of conversion. Both the initial carrier and the carrier after 40 cycles in the fluidized bed are shown.

modified with 5, 10, and 15 wt % K^+ and raw ilmenite. The ilmenites' conversions with time and conversion rates as functions of conversion before and after 40 cycles are presented. Figure 2 clearly shows that, during the entire reduction process, the reactivities of all three types of ilmenite loaded with different amounts of K^+ were enhanced and much faster than that of raw ilmenite. Initially, the ilmenite samples

impregnated with 5, 10, and 15 wt % K^+ presented similar reactivities (2.83%/min on average, as calculated by eq 6) that were about 8.48 times the reactivity of raw ilmenite (0.33%/min). After 40 cycles, the reactivities of both K10-ilmenite and K15-ilmenite increased, whereas a slightly decrease (from 2.83%/min to 2.55%/min) was found for the reactivity of K5-ilmenite. The effect of K^+ loading on improving the reactivity was found to follow the order 15 wt % K^+ > 10 wt % K^+ > 5 wt % K^+ at the end of 40 cycles. Accordingly, the optimum loading mass ratio of K^+ to ilmenite was determined to be 15 wt %. The 40-cycled K15-ilmenite (5.04%/min on average) exhibited a slightly faster reactivity than the 40-cycled K10-ilmenite (4.81%/min on average); however, both of these samples had much faster reactivities than the activated raw ilmenite. The reactivity of the 40-cycled K15-ilmenite was approximately 6.85 times faster than that of the activated raw ilmenite. The conclusion drawn in our previous work that the reactivity of K15-ilmenite was deduced from a simple calculation based on the required bed inventory for complete CO conversion. Therefore, there must be some deviation, which is insignificant. The average reduction rate of activated raw ilmenite (i.e., 40-cycled raw ilmenite) was $\sim 0.74\%/min$ with 11 vol % CO at 900 °C, which is lower than the 2.5%/min obtained by Mendiara et al.²⁸ with 15% CO + 20% CO₂ at 950 °C. This difference might be related to the reaction conditions and the data processing method. Nevertheless, here, we used the reduction rates of 2.5%/min for activated ilmenite and 18.2%/min for a synthetic Ni carrier from the same work of Mendiara et al.²⁸ for comparison. The reactivity of the 40-cycled K15-ilmenite would be 17.13%/min ($6.85 \times 2.5\%/min$) under the condition that the reduction rate of activated ilmenite is 2.5%/min. In this way, the reactivity of the 40-cycled K15-ilmenite can be considered to reach a level equivalent to that of synthetic Ni-based carrier.

The effects of foreign ion type and K^+ loading on the reactivity of ilmenite investigated by TGA in this work are in agreement with those from our previous study using a fluidized bed.²⁷ The most probable mechanisms of the reactivity enhancement of foreign ions proposed in the previous work include (1) the migration of foreign ions (especially K^+ and Na^+), which act as "pore promoters" and (2) the formation of the catalytically active alkali-rich phases, that is, $K_{1.46}Ti_{7.2}Fe_{0.8}O_{16}$ or $Na_2Fe_2Ti_6O_{16}$.²⁷ Ca^{2+} has a low diffusion or migration rate and thus shows a minor effect on enhancing the reactivity. The morphologies observed by SEM previously²⁷ and the Brunauer–Emmett–Teller (BET) surface areas and pore volumes in Table 4 indicate that the porosities of these modified ilmenite particles after 40 cycles fall in the order $K^+ >$

Table 4. BET Surface Areas and Pore Volumes of Raw Ilmenite and Ilmenite Impregnated with 10% K, 10% Na, 10% Ca, 5% K, and 15% K for Samples Extracted from the Fluidized Bed after 40 Redox Cycles

ilmenite	BET surface area (m ² /g)	pore volume ($\times 10^{-6}$ m ³ /kg)
raw	0.32	1.12
10% K	0.45	2.95
10% Na	0.62	1.26
10% Ca	1.84	1.14
5% K	0.36	0.66
15% K	1.27	4.63

$\text{Na}^+ > \text{Ca}^{2+}$ and $15 \text{ wt } \% \text{K}^+ > 10 \text{ wt } \% \text{K}^+ > 5 \text{ wt } \% \text{K}^+$; all the 40-cycled modified ilmenites showed more porous structures than the 40-cycled raw ilmenite and the corresponding initial modified ilmenite. K15-ilmenite gained the best porous structure after 40 cycles, with a surface area and pore volume ~ 4 times larger than that of activated raw ilmenite. These characterizations of microscopic structures present a good explanation for the reactivity differences among the ilmenites tested by TGA, as discussed in sections 4.1 and 4.2. It should be mentioned that, in Table 4, the surface area of Ca10-ilmenite is greater than those of K10- and Na10-ilmenite. This should be attributed to the CaO contained in the Ca10-ilmenite particles, which has a relatively large surface area. During the BET surface area and pore volume tests, considering the nonuniform or heterogeneous structure of the natural ilmenite, each sample tested was about 3 g, which contained quite a number of particles. Also, the test for each type of sample was repeated once. In each test, both the adsorption and desorption processes were analyzed. The results indicated the same trend as reported in Table 4.

In addition to the positive pore-promoting effect of foreign ions K^+ and Na^+ and the formation of active alkali-rich phases, the volatilization of alkali metals causes a fractional loss of K^+ and Na^+ , as shown by the XRF analysis in Table 1. Taking K15-ilmenite as an example, the mass fraction of K remaining in the particle at the end of 40 cycles was only 10% of the combined mass of Ti and Fe, which is 5 times less than that in the initial particles (50%). Based on a previous study,²⁷ this is because of the volatility of the alkali metals under the reaction conditions, along with the chemical combination of alkali-rich phases formed between foreign ions and titanium or iron oxides. However, the volatilization of K^+ from cycle 40 to cycle 100 was negligible. Most of the foreign alkali metals are released during the first several cycles when K_2CO_3 or Na_2CO_3 is transited to the alkali-rich phase. As demonstrated previously, the volatilization of K^+ and Na^+ does not affect the reactivity within 40 cycles;²⁷ the modified ilmenite shows great stability in reactivity after the first several cycles (11 cycles for K15-ilmenite). Because Ca^{2+} is relatively difficult to volatilize, not much loss of Ca^{2+} was found for Ca10-ilmenite. Downstream problems related to the volatilization of alkali metals, such as deposition and corrosion, were addressed previously.²⁷ The alkali-metal volatilization process, which mostly occurs during the transition from K_2CO_3 or Na_2CO_3 to the alkali-rich phase, can be accomplished in a separate laboratory-scale fluidized-bed reactor before participating in the true reaction. Moreover, the released alkali metals can be captured by additives, such as kaolin,³⁹ SiO_2 , MgO , and Al_2O_3 .⁴⁰

4.3. Effect of CO Concentration. According to the results reported in the preceding sections, K15-ilmenite was found to be the best foreign-ion-promoted ilmenite, and therefore, the rest of the study focused on this ilmenite. Fuel gas concentration is one important operational factor. Therefore, different CO concentrations (1, 3, 5, 7, and 11 vol %) were used in this work to investigate the effect of the CO concentration on the enhanced reactivity of the 40-cycled K15-ilmenite in a TGA reactor. Figure 3 shows the conversion of this ilmenite with time and its conversion rate as a function of conversion with the mentioned CO concentrations at 900 °C. It can be seen that, during the entire reduction process, as the CO concentration decreased, the reduction reactivity of the cycled K15-ilmenite became slower. It should be noted that, during the preset 30-min reduction, the dead time required for

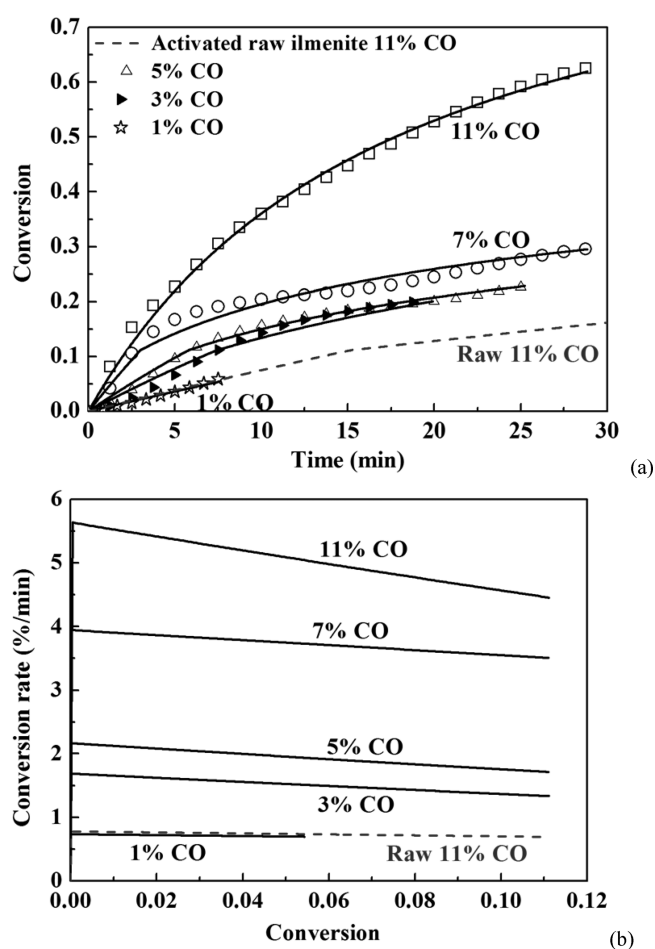


Figure 3. Reduction reactivity of 40-cycled K15-ilmenite with different CO concentrations at 900 °C in a TGA reactor. (a) Conversion of K15-ilmenite with time and (b) conversion rate during the reduction from Fe_2O_3 to Fe_3O_4 ($X_r = 0 \rightarrow 0.11$) in K15-ilmenite as a function of conversion. The reactivity of 40-cycled, activated raw ilmenite with 11 vol % CO at 900 °C is also included for comparison. Solid/dashed lines, calculations; points, experiments.

the reducing gas to travel in the gas pipe and then enter into the TGA reactor increased as the CO concentration decreased, thus shortening the effective reduction time. Therefore, in Figure 3a, the lower CO concentrations correspond to shorter reduction times. The reactivity drops from 5 to 3 vol % CO during the entire reduction and from 11 to 7 vol % CO during the reduction to Fe_3O_4 ($X_r = 0 \rightarrow 0.11$) were not as much as in other situations. Although the reactivity of the 40-cycled K15-ilmenite decreased at lower CO concentrations (< 11 vol %), it was still faster than that of activated raw ilmenite with 11 vol % CO. Even when the CO concentration was decreased to only 1 vol %, the reduction rate of the cycled K15-ilmenite still remained about the same as that of the activated raw ilmenite with 11 vol % CO. Again, as mentioned in section 4.2, the 40-cycled K15-ilmenite had a promoted reactivity, ~ 6.85 times faster than that of the activated raw ilmenite when reduced with 11 vol % CO at 900 °C. In CLC, especially with solid fuels, the fuel gas concentration varies at different locations of the fuel reactor because of both the chemical reaction and the physical fluidizing hydrodynamics, such as mixing or segregation.⁴¹ A high reactivity with varying fuel gas concentrations can ensure a complete fuel gas conversion, producing a high CO_2 concentration at the outlet, and is thus desirable. Conversely,

a low reactivity corresponds to a low CO₂ concentration due to dilution by the unconverted fuel gas. From this aspect, the reactivity-promoted K15-ilmenite is a promising oxygen carrier for CLC technology.

4.4. Effect of Number of Cycles. In a CLC system, oxygen carrier particles recirculate between the interconnected fuel reactor and air reactor until they are elutriated or drained together with the solid-fuel ash. The reactivity of the oxygen carrier changes during successive redox cycles. Therefore, it is necessary to investigate the effect of the number of cycles on the carrier's reactivity. In this section, K15-ilmenite particles that had been subjected to 40, 70, and 100 successive cycles in a laboratory fluidized bed at 900 °C with 11 vol % CO, together with the initial particles, were tested in a TGA reactor at the same temperature and CO concentration. The conversions of these K15-ilmenite samples as a function of time are illustrated in Figure 4. During the entire reduction, the reactivity of K15-

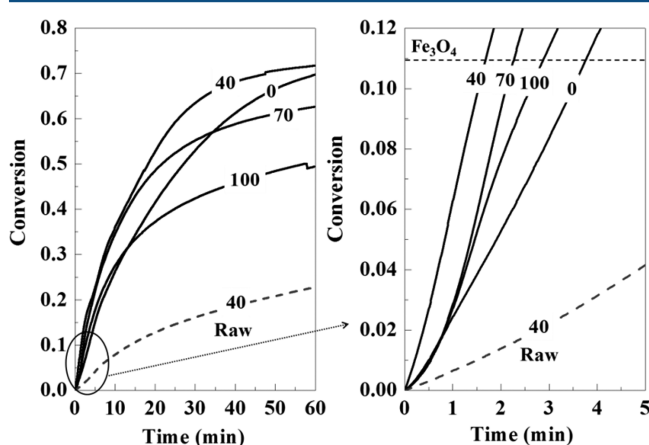


Figure 4. Conversion of K15-ilmenite after different cycles as a function of time with 11 vol % CO at 900 °C in a TGA reactor. The numbers denote the number of cycles that the ilmenite experienced in the fluidized bed with 11 vol % CO at 900 °C. The right graph is an enlarged view of the indicated region in the left graph. The data for 40-cycled raw ilmenite are also shown.

ilmenite after 40 cycles was faster than that of the initial particles. This is in accordance with the previous study,²⁷ where it was found that the reactivity of K15-ilmenite increased during the first 11 cycles and then stabilized from cycle 12 to cycle 40 in the fluidized bed. However, the reactivity of K15-ilmenite after 70 cycles was lower than that after 40 cycles, and it continued to decrease as the number of cycles increased to 100. Although a reactivity decrease occurred for cycles 40–100, the cycled particles still showed higher reactivities than the initial particles in the conversion ranges of 0–0.57 and 0–0.30 for the 70- and 100-cycled K15-ilmenite, respectively. Taking the conversion to Fe₃O₄ ($X_r = 0.11$) as an example, the times required for this conversion were 1.64, 2.21, and 2.81 min for the 40-, 70-, and 100-cycled samples, respectively; all of these times are shorter than the 3.72 min required for the initial material. Furthermore, all of these times in the case of K15-ilmenite were far shorter than the 15.2 min required for the 40-cycled activated raw ilmenite. It can thus be easily calculated that the average reduction rate of the 100-cycle K15-ilmenite (3.91%/min) was 5.29 times higher than that of the 40-cycled raw ilmenite (0.74%/min). Moreover, no evidence of agglomeration was found for the K15-ilmenite particles extracted from the fluidized bed after 40, 70, and 100 cycles.

In fact, the 100-cycled K15-ilmenite maintained a surface area (1.63 m²/g) and pore volume (4.42×10^{-6} m³/kg) similar to those of the 40-cycled K15-ilmenite, whose surface area and pore volume were ~4 times larger than those of the activated raw ilmenite. This further confirms the stability of K15-ilmenite and its feasibility as an oxygen carrier for CLC.

4.5. Application of Reactivity to Design Criteria. The reduction kinetic data obtained were applied for the design of a CLC reactor. Here, we took CO as the fuel gas and assumed that CO was completely converted into CO₂. All of the calculations here are reported per unit fuel power, P_{CO} (1 MW_{th}). The CO mass flow rate, \dot{m}_{CO} , was calculated by dividing the fuel power, P_{CO} , by the CO heating value, LHV (11.8 MJ/kg), giving

$$\dot{m}_{CO} = \frac{P_{CO}}{LHV} = 0.085 \text{ kg/s} \quad (7)$$

The mass flow rate of oxygen required to fully oxidize the CO was obtained according to the equation

$$\dot{m}_O = 2M_{O_2} \frac{\dot{m}_{CO}}{M_{CO}} = 0.048 \text{ kg/s} \quad (8)$$

where M_i denotes the molar mass of species i .

The conversion of ilmenite, X , is defined as the actual mass of oxygen divided by the mass of oxygen when fully oxidized, as given by

$$X = \frac{M_{\text{actual}} - M_r}{M_o - M_r} \quad (9)$$

The average conversion of the oxygen carrier in the air reactor, X_{AR} , was higher than that in the fuel reactor, X_{FR} . The oxidation of the oxygen carrier was generally fast, and thus, we assume that the ilmenite was fully oxidized in the air reactor, that is, $X_{AR} = 1$. In addition, because only the reduction from Fe₂O₃ to Fe₃O₄ gives complete conversion of CO to CO₂, which is suitable for CLC, the most reduced form of the iron oxides in ilmenite is assumed to be Fe₃O₄. X_{FR} varies between 0 (when fully reduced to Fe₃O₄) and 1 (when not reduced). The conversion difference between the two reactors, ΔX , is given by

$$\Delta X = X_{AR} - X_{FR} \quad (10)$$

ΔX also varies in the range of 0–1.

The oxygen capacity of the carrier, C , is defined as the ratio of the fractional mass increase to the increase in conversion, measuring how much oxygen the carrier is able to transfer for a given change in conversion

$$C = \frac{1}{m} \frac{dm}{dx} \quad (11)$$

The oxygen capacity, C , can be manipulated as a function of the conversions in the air and fuel reactors to give

$$C_{AR} = \frac{R_o}{1 - (1 - X_{AR})R_o} \quad (12)$$

$$C_{FR} = \frac{R_o}{1 - (1 - X_{FR})R_o} \quad (13)$$

where R_o is the oxygen ratio of the carrier, defined by eq 4. During the transition from Fe₂O₃ to Fe₃O₄, as assumed, $R_o = 3.33$ wt %. Because it is assumed that $X_{AR} = 1$, $C_{AR} = R_o$. C_{FR} increases as X_{FR} decreases, and the largest C_{FR} value is reached

when $X_{FR} = 0$. This occurs when the iron oxides from ilmenite are fully reduced to Fe_3O_4 in the fuel reactor.

Based on the reduction rate of ilmenite (dX_r/dt) calculated from eq 5, the required solids inventory in the fuel reactor, $m_{bed,FR}$ can be obtained as

$$m_{bed,FR} = \frac{\dot{m}_o}{C_{FR} \frac{dX_r}{dt}} \quad (14)$$

The oxygen carriers of higher reactivity correspond to lower solids inventories required in the fuel reactor, whereas the lower-reactivity carriers require greater solids inventories. At the same time, the solids inventory decreased as the oxygen capacity C_{FR} increased. This suggests that the minimum solids inventory was obtained with the highest C_{FR} value when the iron oxides were in the most reduced state of Fe_3O_4 , namely, $X_{FR} = 0$. It should be noted that reduction rate in eq 14 was evaluated at the average conversion rate during the transition from Fe_2O_3 to Fe_3O_4 , as given by eq 6. This approach thus imposes some limitations on the ensuing predictions.

The solids circulation rate of the oxygen carrier between the two reactors, \dot{m}_{OC} , depends on the conversion difference

$$\dot{m}_{OC} = \frac{\dot{m}_o}{C_{AR} \Delta X} \quad (15)$$

Based on eqs 14 and 15, the 40-cycled foreign-ion-promoted K15-ilmenite and the activated raw ilmenite were compared in terms of the required solids circulation rate and solids inventory of the fuel reactor (FR), as illustrated in Figure 5. As the

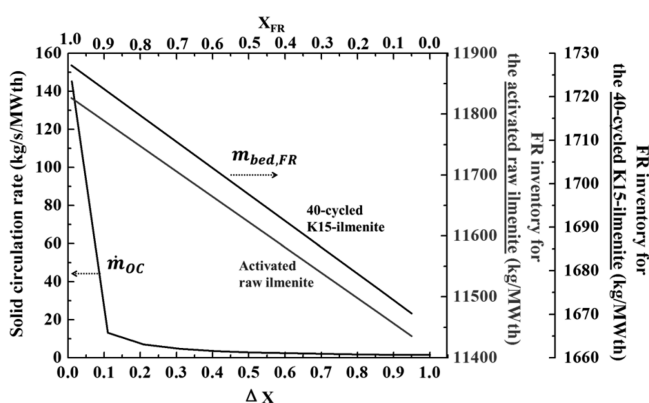


Figure 5. Solids circulation rate \dot{m}_{OC} (kg/s per MW_{th} of CO) and solids inventory of the fuel reactor (FR) $m_{bed,FR}$ (kg per MW_{th} of CO) as functions of the conversion difference ΔX and the conversion in the fuel reactor X_{FR} for both the activated raw ilmenite and the 40-cycled K15-ilmenite.

conversion difference rose, the amount of oxygen transported to the fuel reactor per kilogram of carrier particles increased. Correspondingly, the required solids circulation rate and FR solids inventory decreased. At a given conversion difference, the 40-cycled K15-ilmenite required a far lower (approximately one-seventh) FR solids inventory than the activated raw ilmenite. For example, the required minimum FR solids inventory at $\Delta X = 1$ or $X_{FR} = 0$ was only 1670 kg/ MW_{th} for the 40-cycled K15-ilmenite, but it increased to 11436 kg/ MW_{th} for the activated raw ilmenite. The initial ilmenite required an even larger minimum inventory (25256 kg/ MW_{th} , not plotted in Figure 5), ~15.12 times larger than that of the 40-cycled K15-ilmenite. The much lower solids inventory required for the

cycled K15-ilmenite is attributed to its promoted, much higher reactivity. A small solids inventory indicates that the CLC system can be scaled down with less capital cost. The theoretical predictions based on kinetic data suggest that the 15 wt % K^+ -promoted ilmenite shows great advantages for CLC. It is worth mentioning that the calculations and conclusions here apply only for CO as a fuel; additional work with H_2 , another primary gasification product, is required for solid-fuel CLC.

6. CONCLUSIONS

This work investigated the reduction kinetics of ilmenite carrier impregnated with different types of foreign ions at different mass ratios with CO as the reducing gas in a TGA reactor. The kinetic parameters were applied to predict the required solids circulation rate and solids inventory for a CLC system. The following conclusions can be drawn:

- (1) A kinetic study by TGA further confirmed that impregnating natural ilmenite ore with foreign ions can promote ilmenite's reduction reactivity. Among the three tested foreign ions, namely, K, Na, and Ca, it was found that K can enhance the reduction kinetics of ilmenite most significantly.
- (2) The 15 wt % K^+ -promoted ilmenite was found to have an ~6.85 times faster reactivity after 40 cycles in the fluidized bed than the activated raw ilmenite. This corresponds to a 6.85 times lower solids inventory required for the fuel reactor with a smaller-scale CLC unit.
- (3) A decrease of the CO concentration was found to reduce the reactivity of the 15 wt % K^+ -promoted ilmenite. However, the reduced reactivity of 15 wt % K^+ -promoted ilmenite at low CO concentrations still remained higher than the reactivity of the activated raw ilmenite at high CO concentrations.
- (4) For cycles 40–100, the reactivity of the 15 wt % K^+ -promoted ilmenite decreased with the number of cycles. Even so, this reactivity was still much faster than that of the activated raw ilmenite. A high fuel gas conversion can be ensured with this promoted reactivity.

AUTHOR INFORMATION

Corresponding Author

*Tel.: 86-10-62781741. Fax: 86-10-62770209. E-mail: lizs@mail.tsinghua.edu.cn.

Notes

The authors declare no competing financial interest.

ACKNOWLEDGMENTS

This work was supported by the National Natural Science Foundation of China (51061130535), National Key Basic Research and Development Program (2011CB707301), Tsinghua University Initiative Scientific Research Program, and Program for New Century Excellent Talents in University (NCET-12-0304).

NOMENCLATURE

- C = oxygen capacity of carrier
 C_{CO} = CO concentration (mol/ m^3)
 k = coefficient for chemical reaction rate [$m^3/(mol \cdot s)$]
 LHV = lower heating value
 M_i = molar mass of species i (kg/mol)

m = reaction order
 m_0 = initial mass at time $t = 0$ (kg)
 $m_{\text{bed,FR}}$ = solids inventory in the fuel reactor (kg)
 m_o = mass of the most oxidized form of the ilmenite (kg)
 m_r = mass of the most reduced form of the ilmenite (kg)
 m_t = mass at time t (kg)
 \dot{m}_{CO} = CO mass flow rate (kg/s)
 \dot{m}_{O} = mass flow rate of oxygen (kg/s)
 \dot{m}_{OC} = solids circulation rate of the oxygen carrier (kg/s)
 n = parameter describing the change in surface area
 P_{CO} = fuel power (MW_{th})
 R_o = oxygen ratio of the carrier
 S_0 = initial surface area of the oxygen carrier particle (m^2)
 Δt = period of time (s)
 X = conversion of the oxygen carrier
 X_{AR} = conversion of the oxygen carrier in the air reactor
 X_{FR} = conversion of the oxygen carrier in the fuel reactor
 X_r = conversion of the ilmenite carrier during reduction by TGA
 $\frac{dX_r}{dt}$ = conversion rate of the oxygen carrier (1/s)
 $\bar{\frac{dX_r}{dt}}$ = average conversion rate of the oxygen carrier (1/s)
 ΔX = conversion difference between the two reactors

REFERENCES

- (1) Richter, H.; Knoche, K. Reversibility of combustion processes. *ACS Symp. Ser.* **1983**, 235, 71.
- (2) Ishida, M.; Jin, H. CO_2 recovery in a power plant with chemical looping combustion. *Energy Convers. Manage.* **1997**, 38, S187.
- (3) Lyngfelt, A.; Thunman, H. Construction and 100 h of operational experience of a 10 kW chemical-looping combustor. In *The CO_2 Capture and Storage Project (CCP) for Carbon Dioxide Storage in Deep Geologic Formations for Climate Change Mitigation*; Elsevier Science: London, 2005; Vol. 1, Chapter 36.
- (4) Markström, P.; Lyngfelt, A. Designing and operating a cold-flow model of a 100 kW chemical-looping combustor. *Powder Technol.* **2012**, 222, 182.
- (5) Kolbitsch, P.; Bolhar-Nordenkamp, J.; Proll, T.; Hofbauer, H. Operating experience with chemical looping combustion in a 120 kW dual circulating fluidized bed (DCFB) unit. *Int. J. Greenhouse Gas Control* **2010**, 4, 180.
- (6) Galloy, A.; Strohle, J.; Eppe, B. Design and operation of a 1 MWth carbonate and chemical looping CCS test rig. *VGB PowerTech* **2011**, 91, 64.
- (7) Andrus, H.; Chui, J.; Thibeault, P.; Edberg, C.; Turek, D.; Kenney, J.; Abdulally, I.; Chapman, P.; Kang, S.; Lani, B. Alstom's limestone-based chemical looping process. Presented at the 2nd International Conference on Chemical Looping, Darmstadt, Germany, Sep 26–28, 2012.
- (8) Shulman, A.; Linderholm, C.; Mattisson, T.; Lyngfelt, A. High reactivity and mechanical durability of $\text{NiO}/\text{NiAl}_2\text{O}_4$ and $\text{NiO}/\text{NiAl}_2\text{O}_4/\text{MgAl}_2\text{O}_4$ oxygen carrier particles used for more than 1000 h in a 10 kW CLC reactor. *Ind. Eng. Chem. Res.* **2009**, 48, 7400.
- (9) Kolbitsch, P.; Bolhar-Nordenkamp, J.; Proll, T.; Hofbauer, H. Comparison of two Ni-based oxygen carriers for chemical looping combustion of natural gas in 140 kW continuous looping operation. *Ind. Eng. Chem. Res.* **2009**, 48, 5542.
- (10) de Diego, L. F.; García-Labiano, F.; Gayán, P.; Celaya, J.; Palacios, J. M.; Adanez, J. Operation of a 10 kWth chemical-looping combustor during 200 h with a $\text{CuO}-\text{Al}_2\text{O}_3$ oxygen carrier. *Fuel* **2007**, 86, 1036.
- (11) Lyngfelt, A. Oxygen carriers for chemical-looping combustion—Operational experience. Presented at the First International Conference on Chemical Looping, Lyon, France, Mar 17–19, 2010.
- (12) Gu, H.; Shen, L.; Xiao, J.; Zhang, S.; Song, T. Chemical looping combustion of biomass/coal with natural iron ore as oxygen carrier in a continuous reactor. *Energy Fuels* **2011**, 25, 446.
- (13) Xiao, R.; Song, Q.; Song, M.; Lu, Z.; Zhang, S.; Shen, L. Pressurized chemical-looping combustion of coal with an iron ore-based oxygen carrier. *Combust. Flame* **2010**, 157, 1140.
- (14) Leion, H.; Jerndal, E.; Steenari, B. M.; Hermansson, S.; Israelsson, M.; Jansson, E.; Johnsson, M.; Thunberg, R.; Vadenbo, A.; Mattisson, T.; Lyngfelt, A. Solid fuels in chemical-looping combustion using oxide scale and unprocessed iron ore as oxygen carriers. *Fuel* **2009**, 88, 1945.
- (15) Linderholm, C.; Lyngfelt, A.; Cuadrat, A.; Jerndal, E. Chemical-looping combustion of solid fuels—Operation in a 10 kW unit with two fuels, above-bed and in-bed fuel feed and two oxygen carriers, manganese ore and ilmenite. *Fuel* **2012**, 102, 808.
- (16) Wen, Y.; Li, Z.; Xu, L.; Cai, N. Experimental study of natural Cu ore particles as oxygen carriers in chemical looping with oxygen uncoupling (CLOU). *Energy Fuels* **2012**, 26, 3919.
- (17) Leion, H. Use of ores and industrial products as oxygen carriers in chemical-looping combustion. *Energy Fuels* **2009**, 23, 2307.
- (18) Mendiara, T.; Abad, A.; de Diego, L. F.; García-Labiano, F.; Gayán, P.; Adanez, J. Use of an Fe-based residue from alumina production as an oxygen carrier in chemical-looping combustion. *Energy Fuels* **2012**, 26, 1420.
- (19) Adanez, J.; Cuadrat, A.; Abad, A.; Gayán, P.; de Diego, L. F.; García-Labiano, F. Ilmenite activation during consecutive redox cycles in chemical-looping combustion. *Energy Fuels* **2010**, 24, 1402.
- (20) Abad, A.; Adanez, J.; Cuadrat, A.; García-Labiano, F.; Gayán, P.; de Diego, L. F. Kinetics of redox reactions of ilmenite for chemical-looping combustion. *Chem. Eng. Sci.* **2011**, 66, 689.
- (21) Leion, H.; Lyngfelt, A.; Johansson, M.; Jerndal, E.; Mattisson, T. The use of ilmenite as an oxygen carrier in chemical-looping combustion. *Chem. Eng. Res. Des.* **2008**, 86, 1017.
- (22) Aziz, M. M.; Jerndal, E.; Leion, H.; Mattisson, T.; Lyngfelt, A. On the evaluation of synthetic and natural ilmenite using syngas as fuel in chemical-looping combustion (CLC). *Chem. Eng. Res. Des.* **2010**, 88, 1505.
- (23) Cuadrat, A.; Abad, A.; García-Labiano, F.; Gayán, P.; de Diego, L. F.; Adanez, J. The use of ilmenite as oxygen carrier in a 500 W_{th} chemical-looping coal combustion unit. *Int. J. Greenhouse Gas Control* **2011**, 5, 1630.
- (24) Berguerand, N.; Lyngfelt, A. Batch testing of solid fuels with ilmenite in a 10 kWth chemical-looping combustor. *Fuel* **2010**, 89, 1749.
- (25) Bidwe, A. R.; Mayer, F.; Hawthorne, C.; Charitos, A.; Schuster, A.; Scheffknecht, G. Use of ilmenite as an oxygen carrier in chemical looping combustion—Batch and continuous dual fluidized bed investigation. *Energy Proc.* **2011**, 4, 433.
- (26) Markström, P.; Lyngfelt, A.; Linderholm, C. Chemical looping combustion in a 100 kW unit for solid fuels. Presented at the 21st International Conference on Fluidized Bed Combustion, Naples, Italy, Jun 3–6, 2012.
- (27) Bao, J.; Li, Z.; Cai, N. Promoting the reduction reactivity of ilmenite by introducing foreign ions in chemical looping combustion. *Ind. Eng. Chem. Res.* **2013**, 52, 6119.
- (28) Mendiara, T.; Pérez, R.; Abad, A.; de Diego, L. F.; García-Labiano, F.; Gayán, P.; Adanez, J. Low-cost Fe-based oxygen carrier materials for the iG-CLC process with coal. 1. *Ind. Eng. Chem. Res.* **2012**, 51, 16216.
- (29) Leion, H.; Mattisson, T.; Lyngfelt, A. Solid fuels in chemical-looping combustion. *Int. J. Greenhouse Gas Control* **2008**, 2, 180.
- (30) Yang, J.; Cai, N.; Li, Z. Hydrogen production from the steam–iron process with direct reduction of iron oxide by chemical looping combustion of coal char. *Energy Fuels* **2008**, 22, 2570.
- (31) Li, F.; Sun, Z.; Luo, S.; Fan, L. Ionic diffusion in the oxidation of iron—Effect of support and its implications to chemical looping applications. *Energy Environ. Sci.* **2011**, 4, 876.
- (32) Adanez, J.; Abad, A.; García-Labiano, F.; Gayán, P.; de Diego, L. F. Progress in chemical-looping combustion and reforming technologies. *Prog. Energy Combust. Sci.* **2012**, 38, 215.
- (33) Ryu, H. J.; Bae, D. H.; Han, K. H.; Lee, S. Y.; Jin, G. T.; Choi, J. H. Oxidation and reduction characteristics of oxygen carrier particles

and reaction kinetics by unreacted core model. *Korean J. Chem. Eng.* **2001**, *18*, 831.

(34) García-Labiano, F.; de Diego, L. F.; Adánez, J.; Abad, A.; Gayán, P. Temperature variations in the oxygen carrier particles during their reduction and oxidation in a chemical-looping combustion system. *Chem. Eng. Sci.* **2005**, *60*, 851.

(35) Bhatia, S. K.; Perlmutter, D. D. Effect of the product layer on the kinetics of the CO₂–lime reaction. *AIChE J.* **1983**, *29*, 79.

(36) Liu, W.; Dennis, J. S.; Sultan, D. S.; Redfern, S. A. T.; Scott, S. A. An investigation of the kinetics of CO₂ uptake by a synthetic calcium based sorbent. *Chem. Eng. Sci.* **2012**, *69*, 644.

(37) Hossain, M. M.; de Lasa, H. I. Reactivity and stability of Co–Ni/Al₂O₃ oxygen carrier in multicycle CLC. *AIChE J.* **2007**, *53*, 1817.

(38) Bao, J.; Li, Z.; Sun, H.; Cai, N. Experiment and rate equation modeling of Fe oxidation kinetics in chemical looping combustion. *Combust. Flame* **2013**, *160*, 808.

(39) Tran, K. Q.; Iisa, K.; Hagström, M.; Steenari, B. M.; Lindqvist, O.; Pettersson, J. B. C. On the application of surface ionization detector for the study of alkali capture by kaolin in a fixed bed reactor. *Fuel* **2004**, *83*, 807.

(40) Sun, D.; Sung, W.; Chen, R. The release behavior of potassium and sodium in the biomass high-temperature entrained-flow gasification. *Appl. Mech. Mater.* **2011**, *71–78*, 2434.

(41) Bao, J.; Li, Z.; Cai, N. Experiments of char particle segregation effect on the gas conversion behavior in the fuel reactor for chemical looping combustion. *Appl. Energy*, published online Jun 11, 2013, 10.1016/j.apenergy.2013.04.086.